博士（人間生物学）

Ph.D. in Human Biology

学位論文

Dissertation

Investigation of Sleep/Wake Regulatory Mechanisms Through the *Sik3* Gene Identified by Forward Genetics

フォワード・ジェネティクスにより同定した新規睡眠覚醒制御遺伝子 *Sik3* の解析による睡眠覚醒制御機構の解明

2017

平成 29 年度

筑波大学　グローバル教育院

ヒューマンバイオロジー学位プログラム

School of Integrative and Global Majors in University of Tsukuba

Ph.D. Program in Human Biology

本多 隆利

Takato Honda

Table of Contents

Table of Figures

Abstract

The mechanism for homeostatic sleep/wake regulation and the neural substrate for “sleepiness” remain among the biggest mysteries in sleep biology. To make a breakthrough in this issue, our laboratory has initiated a large-scale forward genetic screen of sleep/wake abnormalities in mice based on somnographic (electroencephalography (EEG)/electromyography (EMG)) measurements, which are the gold standard in mammalian sleep/wake assessment. We have so far screened > 8,000 heterozygous ENU-mutagenized mice and established multiple pedigrees exhibiting heritable and specific sleep/wake abnormalities. By combining linkage analysis and whole-exome sequencing, we have identified two dominant mutations that strongly affect sleep/wakefulness (Funato H, Honda T, Yanagisawa M et al., *Nature* 2016). A splicing mutation in the *Sik3* protein kinase gene (termed *Sleepy* mutation) causes marked hypersomnia (i.e., increased non-REM sleep (NREMS)) due to an increase in inherent sleep

need. A missense mutation in the sodium leak channel NALCN (termed *Dreamless* mutation) reduces both the total amount and episode duration of REM sleep, apparently by increasing the excitability of REM sleep-inhibiting neurons. Since these dominant mutations cause severe and specific sleep abnormalities, we expect that the mutated genes play central roles in regulating sleep/wake amounts.

To elucidate the molecular basis of how the *Sik3* gene is involved in sleep/wake regulation, we performed genetic and biochemical analyses. SIK3 has a serine-threonine kinase domain at the N terminus and a protein kinase A (PKA) recognition site (Ser551) in the middle portion. The skipping of exon 13 resulted in an in-frame deletion of 52 amino acids (*ΔEx13*, termed *Sleepy* mutation) encompassing Ser551, a PKA recognition site. Thus, we hypothesized that Ser551 of *Sik3* has an essential role for the regulation of daily sleep amount and sleep need. To examine this hypothesis, we generated the transgenic mice with Ser551Ala substitution (termed *S551A* mutant) and Ser551Asp substitution (termed *S551D* mutant)

by CRISPR/Cas9 system.

As a result, *S551A* and *S551D* mutant mice both exhibited longer NREMS and decreased wakefulness, similar to the phenotype of the exon skipped *Sleepy* (*ΔEx13*) mutant. Moreover, both *S551A* and *S551D* mutant mice exhibited increased density of slow-wave activity during NREMS and increased individual NREMS episode durations, suggesting that the baseline sleep need is inherently increased in the mutants. To elucidate the mechanism of their sleep/wake phenotypes with prolonged NREMS, we performed biochemical analyses by using a series of expression plasmids (WT, *Sleepy* (*ΔEx13*), *S551A*, *S551D*) to examine how the mutations at Ser551 affect the signaling pathway and binding partners of SIK3. Through immunoprecipitation and western blotting, we confirmed that in *Sleepy* (*ΔEx13*), *S551A*, and *S551D*, all the mutants showed decreased binding to phospho-PKA substrate antibody. This result strongly suggests that the SIK3 protein with the mutations *S551A*, *S551D* and *Sleepy* (*ΔEx13*) is excluded from the possible substrates of PKA. Together, these three

mutants showed abolished bindings toward 14-3-3, which corresponded to their consistent hypersomnia phenotypes with prolonged NREMS.

These results suggest that the existence of Ser551 in the *Sik3* gene and its signaling pathway, including PKA and 14-3-3, may play a key role in sleep/wake regulation under normal physiological conditions. Notably, the exon 13-encoded region of *Sik3*, including Ser551, is highly conserved among both vertebrates and invertebrates, which suggests the biological importance of the phosphorylation pathway PKA / SIK3 / 14-3-3 in sleep/wake regulation. These findings provide landmark information about the novel sleep/wake regulatory mechanisms by connecting the intracellular signaling pathway to the dynamic *in vivo* sleep/wake behaviors.

Introduction

Prologue

The applicant's previous research elucidated the minimal neural circuit responsible for olfactory associative memory in *Drosophila* larvae. Our study showed that the optogenetic and thermogenetic activation of both single olfactory receptor neurons and octopaminergic neurons were sufficient for the formation of associative olfactory memory in the larval brain (Honda T et al., *Scientific Reports*, 2014; Honda T et al., *Frontiers in Behavioral Neuroscience* 2016). Based on this research, the applicant became interested in the roots of behaviors and how information processing in defined neural circuits and genes generates complex animal behaviors. This experience drove the applicant to become interested in approaching a mysterious and conserved behavior across species: "sleep".

We human beings spend nearly one-third of our lives asleep. However,

the mechanism and function of sleep remain unclear. Understanding the mechanisms of homeostatic sleep has not only a biological significance but also a great benefit for human society. In Japan in particular, it has been reported that the economic losses reach 3.5 trillion yen per year due to people's troubles with sleep (Uchiyama M. *J Jpn Psychiatr Hosp Assoc* 2012). Sleep disorders have deep relationships with metabolic syndromes and with mental disorders such as depression and dementia. It is thus necessary to decode the mystery of sleep/wake mechanisms and develop a way to control sleep/wake.

As the largest unrevealed issue in sleep biology, the mechanism for homeostatic sleep/wakefulness regulation and the neural substrate for "sleepiness" remain a mystery. A homeostatic sleep need is represented as the "integrator" of the recent history of the time spent in sleep. The EEG spectral power in the delta-range frequency (1–4 Hz) during NREMS has been considered a marker of sleep need. Although a number of studies have shown the executive neural circuitries regulating sleep/wake, the molecular

mechanisms that determine the propensity of switching between wakefulness, REMS and NREMS remain unknown. Therefore, we decided to apply a phenotype-driven forward-genetics approach that is free from specific working hypotheses (Takahashi JS, et al. *Science* 2008).

History of forward genetics

Historically, forward genetics made a significant contribution for the discoveries of molecular mechanisms controlling the circadian rhythm. In 1971, Dr. Benzer and Dr. Konopka randomly mutagenized approximately 2,000 fruit flies and found a *Period* mutant with abnormal circadian rhythm (Benzer and Kopnoka. *PNAS* 1971). Dr. Hall's and Dr. Rosbash's group and Dr. Young identified its causative gene *period* (Reddy P, et al. *Cell* 1984; Zehring WA, et al. *Cell* 1984; Bargiello TA, et al. *Nature* 1984). As the second identified clock gene, in 1973, Dr. Hoyle's group isolated the circadian clock mutants of *Neurospora crassa* and found the *frequency*

mutant (Feldman JF, et al. *Genetics* 1973); Dr. Dunlap and his colleagues later identified the responsible gene *frequency* (McClung CR, et al. *Nature* 1989). Dr. Takahashi used forward genetics in mice and identified *Clock* gene as the first report of mammalian clock gene (Vitaterna MH, et al. *Science* 1994; King DP, et al. *Cell* 1997). With the discovery of *Clock* gene, the fundamental principle of a circadian oscillator formed by transcriptional feedback loop was beautifully revealed. This history shows that the research field of circadian rhythm was driven and developed by the power of forward genetics.

Forward genetics in sleep studies

By contrast with circadian regulation, sleep has the unique characteristics of effective compensation and redundancy. In mammalian species, sleep has a relatively clear definition based on EEG and EMG that allows us to evaluate wakefulness, NREMS, and REMS status. However, it

is technically hard to adapt this criteria for animals such as invertebrate species, in which EEG/EMG recording cannot be applied. Thus, for examining sleep-like behaviors across animal species, the following criteria have been reported: 1) loss of locomotion, 2) enhanced arousal thresholds to environmental stimuli, 3) rapid reversibility, and 4) homeostasis via sleep rebound (Campbell SS and Tobler I. *Neurosci Biobehav Rev* 1984; Rial RV, et al. *Neurosci Biobehav Rev* 2010). In 2000, Dr. Hendricks, Dr. Pack and Dr. Tononi's research groups reported sleep-like behavior that met the criteria described above in the fruit fly *Drosophila* (Hendricks JC, et al. *Neuron* 2000; Shaw PJ, et al. *Science* 2000). Dr. Danilova's team reported sleep-like behavior in zebrafish (Zhdanova IV, et al. *Brain Res* 2001). Recently, it has been reported that the jellyfish, *Cassiopea,* which does not have a centralized nervous system, also exhibited sleep-like behavior (Nath RD, et al. *Curr Biol* 2017). In 2005, Dr. Tononi's group applied the forward genetics approach to approximately 9,000 fruit flies and identified the *minisleep* mutant, which presents the strong phenotype of

a sleep amount that is 1/3 that of wild-type flies. They identified the responsible gene, *Shaker,* that coded the K^+ channel (Cirelli C, et al. *Nature* 2005). In the same year, Dr. Kume and his colleagues isolated the *fumin* mutant fly with a short sleep phenotype. They reported that the *fumin* mutant had a deletion mutation in *dopamine transporter (DAT)* gene (Kume K, et al. *J Neurosci* 2005). Dr. Sehgal's group screened approximately 3,500 mutant flies bearing transposon insertions and identified the *sleepless (sss)* mutant. They showed that the *sss* gene encoded the glycosyl-phosphatidylinositol (GPI)-anchored membrane protein (Koh K, et al. *Science* 2008). Dr. Raizen and Dr. Pack demonstrated that the cGMP-dependent protein kinase (PKG) coding gene *elg-4* had a key role on sleep-like behavior termed "lethargus" in *C. elegans* (Raizen DM, et al. *Nature* 2008).

Forward genetics of sleep in randomly mutagenized mice

Forward genetics has also contributed greatly to the sleep research field. However, the sleep/wake regulating genes identified in invertebrates are not always conserved in mammals, including humans. In addition, the behavioral and locomotor based criteria do not allow us to distinguish between the states of quiet wakefulness and actual sleep.

To achieve a breakthrough on this issue, we have initiated a large-scale forward genetic screen of sleep/wake phenotype in mice, based on true somnographic (EEG/EMG) measurements, which are the gold standard in mammalian sleep/wake assessment. To date, we have screened > 8,000 heterozygous ENU-mutagenized mice and established multiple pedigrees exhibiting heritable and specific sleep/wake abnormalities. By combining linkage analysis and whole-exome sequencing, we have identified and reported two dominant mutations that strongly affect sleep/wakefulness (Funato H, Honda T, Yanagisawa M, et al. *Nature* 2016). A splicing mutation in the *Sik3* protein kinase gene (termed *Sleepy* mutation) causes marked hypersomnia (increased non-REM sleep) due to an increase in

inherent sleep need. A missense mutation in the sodium leak channel NALCN (termed *Dreamless* mutation) reduces both the total amount and episode duration of REM sleep, apparently by increasing the excitability of REM sleep-inhibiting neurons. Since these dominant mutations cause severe and specific sleep abnormalities, we expect that the mutated genes play central roles in regulating sleep/wake amounts.

Research strategy for elucidating sleep/wake regulatory mechanisms

To elucidate the molecular basis of how the *Sik3* gene is involved in sleep/wake regulation, we performed the genetic and biochemical analyses described in this study. Notably, SIK3 has a serine-threonine kinase domain at the N terminus and a protein kinase A (PKA) recognition site (Ser551) in the middle portion. The skipping of exon 13 resulted in an in-frame deletion of 52 amino acids (*ΔEx13*, termed *Sleepy* mutation) encompassing Ser551, a PKA recognition site. Thus, we hypothesized that Ser551 of *Sik3*

has an essential role for the regulation of daily sleep amount and sleep need. To examine this hypothesis, we generated the transgenic mice with Ser551Ala substitution (termed *S551A* mutant) and Ser551Asp substitution (termed *S551D* mutant) by CRISPR/Cas9 system (Figure 1).

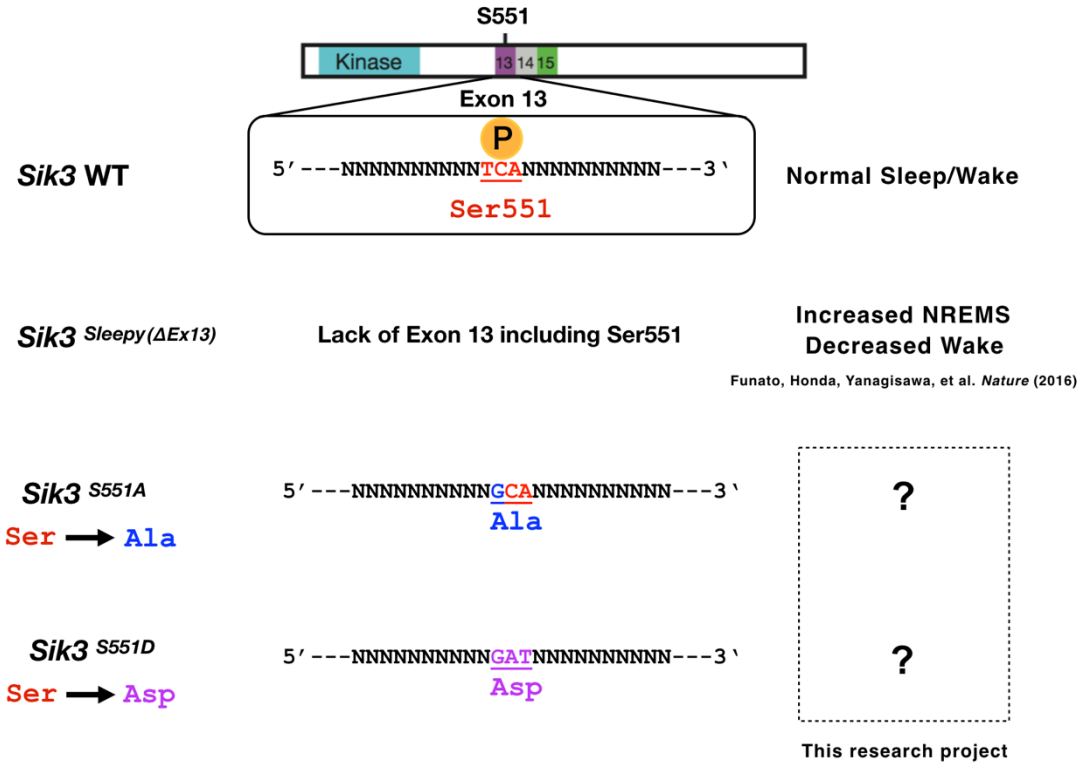

Figure 1. Generation of *S551A* and *S551D* mutant mice pedigree

Materials and Methods

Animals. *S551A* and *S551D* mutant mice and littermate wildtype mice were maintained on a C57BL/6 background. Mice were housed under a 12:12-hr light/dark cycle and controlled temperature and humidity conditions. Food and water were delivered ad libitum. When the mice were under EEG/EMG recording, a water gel pack (Napa Nector, 8 oz., System Engineering Lab Group Inc.) was used for a water source to intake water easily. All procedures were approved by the Institutional Animal Care and Use Committee of the University of Tsukuba.

Generation of *S551A* and *S551D* mutant mice by CRISPR/Cas9 system. To construct a Cas9/single-guide RNA (sgRNA) expression vector, oligonucleotide DNAs (For both *S551A/D*: 5′-caccggccggagagcctcagatgg-3′ and 5′-aaacccatctgaggctctccggcc-3′) were annealed and inserted into pX330 vector (Addgene). Based on the EGxxFP system (Mashiko D, et al.

Scientific Reports 2013), the cleavage activity of the pX330-S551A/D vector was verified in cultured cells (Figure 2). Genomic DNA containing exon 13 (including Ser551 in the center) of the *Sik3* gene was amplified and inserted into pCAG-EGxxFP to produce pCAG-EGxxFP-*Sik3*Ex13 using In-Fusion HD Cloning Kit (TaKaRa). The pX330-S551A/D and pCAG-EGxxFP-*Sik3*Ex13 were transfected into HEK293 cells with Lipofectamine LTX (ThermoFisher). The EGFP expression was evaluated 48 hours after transfection (Figure 2). As a donor oligonucleotide to induce the amino acid change, a single-stranded 200-nucleotide DNA was synthesized (Integrated DNA Technologies), which contained a Ser551Ala or Ser551Asp coding sequence in the center and 99-nucleotide arms at the 5′ and 3′ ends. Female C57BL/6J mice were injected with pregnant mare serum gonadotropin (PMSG) and human chorionic gonadotropin (hCG) at a 48-h interval and were then mated with male C57BL/6J mice. The fertilized one-cell embryos were collected from the oviducts. Subsequently, 5 ng μl^{-1} of pX330-S551A/D vector and 10 ng μl^{-1} of the donor

oligonucleotide were injected into the pronuclei of these one-cell embryos. The injected one-cell embryos were transferred into pseudopregnant ICR mice. F0 mice were genotyped for the presence of *S551A* or *S551D* mutation in exon13 of the *Sik3* gene. F0 mice were checked for the absence of the Cas9 transgene and off-target effects. Candidate off-target sites were identified based on a complete match of S551A/D 16 bp target sequence (gagcctcagatggagg), including the PAM sequence. F0 mice were mated with the counter C57BL/6N mice to obtain F1 offspring.

Quantitative RT-PCR. Total RNA was extracted from tissue sample using the RNeasy Lipid Tissue Mini kit (Qiagen) and QiAzol Lysis Reagent (Qiagen). cDNA was synthesized with oligo dT primers using a PrimeScript reverse transcriptase kit (TaKaRa). Real-time quantitative PCR reactions were performed with ViiA7 Real-Time PCR System (ThermoFisher) using SYBR GREEN PreMix Ex Taq (TaKaRa). The averages of *glyceraldehyde-3-phosphate dehydrogenase* (GAPDH) mRNA

were used for normalization. The following PCR primers were used: *Gapdh* forward, 5′-agaacatcatccctgcatcc-3′; *Gapdh* reverse, 5′-cacattgggggtaggaacac-3′; *Sik3* forward, 5’-ttgtcaatgaggaggcacac-3’; *Sik3* reverse, 5’-tgttaggggccacttgtagg-3’. For the RT-PCR experiment in Figure 4, the following PCR primers were used: *Sik3* forward, 5′-catccacaggggtaactgct-3′; *Sik3* reverse 5′-gaacagatctgcaggcacaa-3′.

Western blot and immunoprecipitation. Brain tissues were homogenized using a homogenizer (Polytron) in ice-cold lysis buffer [20 mM HEPES, pH 7.5, 100 mM NaCl, 10 mM $Na_4P_2O_7$, 1.5% Triton X-100, 15 mM NaF, 1×PhosSTOP (Roche), 5 mM EDTA, 1×protease inhibitor (Roche)] and then centrifuged at 13,000 g at 4 °C. The supernatants were separated by SDS–PAGE and transferred on PVDF membrane. Cultured cell lysates were prepared with ice-cold lysis buffer [1 M HEPES-NA, pH 7.5, 5 M NaCl, 0.1 M $Na_4P_2O_7$, 10% Triton X-100, 0.5 M NaF, 10×PhosSTOP (Roche), 0.5 M EDTA, 25×proteases inhibitor EDTA (Roche)], rotated > 15

min at 4 °C, and centrifuged at 13,000 g at 4 °C. Western blotting was performed according to standard protocols using the corresponding antibodies (see also “Antibodies” section). Immunoprecipitation (IP) was performed for the HA-tagged SIK3 proteins (HA-*Sik3* (WT), HA-*S551A*, HA-*S551D* and HA-*Sleepy* (*ΔEx13*)) using HA tagged Protein Purification Kit (MBL 3325).

Antibodies. Anti-SIK3 (C-terminal) antibody: a rabbit polyclonal antibody against the C-terminal 171 amino-acids of mouse SIK3 was generated using custom antibody production service. Anti-SIK3 (Ex13) antibody: a rabbit polyclonal antibody against 14 amino acids of mouse SIK3 Exon 13 (LHAQQLLKRPRGPS) was generated using a custom antibody production service. Anti-phospho-PKA substrate (RRXS/T) (100G7E) antibody: a rabbit monoclonal antibody against pPKA substrate (Cell Signaling). Anti-14-3-3 (pan) antibody: a rabbit polyclonal antibody detects all known isoforms of mammalian 14-3-3 proteins (Cell Signaling).

Anti-HA-Tag (C29F4) antibody: a rabbit monoclonal antibody against HA-tag (Cell Signaling). Antiβ-Tubulin (9F3) antibody: a rabbit monoclonal antibody as a loading marker (Cell Signaling).

Plasmid constructs. HA-tagged *Sik3* cDNA were subcloned into pcDNA3.1 vectors using an In-Fusion HD Cloning kit (TaKaRa). The nucleotide substitutions (*ΔEx13/S551A/S551D*) were introduced into HA-tagged *Sik3* cDNA using a KOD-Plus-Mutagenesis kit (Toyobo) and a PrimeSTAR Mutagenesis Basal Kit (TaKaRa).

Cell culture and transfection. HEK293 cells were cultured in DMEM with 10% fetal bovine serum and penicillin/streptomycin. For plasmid transfection, HEK293 cells were grown to 80% confluency in 6-well plates. HEK293 cells were transfected with 500 ng pcDNA constructs encoding HA-*Sik3* (WT), HA-*Sleepy* (*ΔEx13*), HA-*S551A* and HA-*S551D* (see also "Plasmid constructs" section) using FuGENE HD Transfection Regent

(Promega) 1.5 μl.

EEG/EMG electrode implantation surgery. EEG/EMG electrodes with 4 EEG electrode pins and 2 EMG wires were implanted in the mice under anesthesia using isoflurane (3% for induction, 1% for maintenance). The coordination of EEG electrodes was set over the frontal and occipital cortices [anteroposterior (AP): 0.5 mm, mediolateral (ML): 1.3 mm, dorsoventral (DV): −1.3 mm; and AP: −4.5 mm, ML: 1.3 mm, DV: −1.3 mm]. The 2 wires for EMG recording were inserted in the neck muscles and subsequently attached to the skull using dental cement. All mice were allowed 7 days to recover from surgery. After recovery, for habituation to the recoding conditions, the mice were tethered to a counterbalanced arm (Instech Laboratories) that allowed free movement and exerted minimal weight for at least 3 days before the recording session. In this study, *Sik3*$^{+/+}$, *Ski3*$^{S551A/+}$, *Sik3*$^{flag,\ S551A/+}$, *Sik3*$^{S551D/+}$ mice were subjected to surgery and EEG/EMG recordings.

Sleep behavior analysis. EEG/EMG signals were recorded for 2 consecutive days from the onset of the light phase to examine sleep/wake behavior under baseline conditions. The recording room was kept under a 12-h light:12-h dark cycle and at a constant temperature (24–25 °C). EEG/EMG data were analyzed using a MatLab (MathWorks)-based, custom semi-automated staging program that allowed the classification of NREMS, REMS, or wakefulness based on a 20-s epoch time window. Wakefulness was scored based on the criteria of the presence of fast EEG, high amplitude and variable EMG. NREMS was staged based on high amplitude, delta (1–4 Hz) frequency EEG and low EMG tonus. REMS was characterized by theta (6–9 Hz)-dominant EEG and EMG atonia. EEG signals were subjected to fast Fourier transform analysis from 1 to 30 Hz with 1–Hz bin using MatLab-based custom software. The hourly delta density during NREMS indicates the hourly averages of delta density, which is the ratio of delta power (1–4 Hz) to total EEG power (1–30 Hz) at each 20-s epoch or all epochs. Based on the normalized method described

in Bjorness TE, et al. *J Neurosci* (2016), the EEG power of sleep/wake status in each frequency bin was normalized to the last half high frequency range (16-30 Hz).

Statistics. Statistical analysis was performed using Graph Pad Prism 7.0 (GraphPad Software) and SigmaPlot 13.0 (Systat Software). All data were subjected to D'Agostino-Pearson (Omnibus K2) normality test for Gaussian distribution and variance. For the data set that showed a Gaussian distribution ($P > 0.05$ in normality test), we performed parametric tests such as two-tailed unpaired *t*-test and ANOVA followed by Bonferroni's multiple comparisons. For the data set that failed to show a Gaussian distribution, we performed non-parametric test such as Mann-Whitney *U*-test. Significance levels in the figures are represented as $P < 0.05$ (*), $P < 0.01$ (**), $P < 0.001$ (***), and $P < 0.0001$ (****). Error bars in the graphs represent as mean ± standard errors of means (SEM).

Results

Verification of CRISPR vector for *S551A* and *S551D* mutations

To generate *S551A* and *S551D* mutant mice using the CRISPR/Cas9 system, we first evaluated the cleavage activity of pX330-S551A/D vector based on the EGxxFP system (Mashiko D, et al. *Scientific Reports* 2013). pX330-S551A/D and pCAG-EGxxFP-*Sik3*Ex13 were transfected into HEK293 cells. The expression of EGFP was evaluated 48 hours after transfection (Figure 2). We confirmed that both double-strand break (DSB) and homology-directed repair (HDR) occurred and that EGFP expression was detected only in the presence of both pX330-S551A/D and pCAG-EGxxFP-*Sik3*Ex13 vectors (Figure 2). Based on this result, we used the verified pX330-S551A/D vector and the donor oligonucleotide inducing the *S551A* or *S551D* mutations for the next micro-injection step to generate the *S551A* and *S551D* mutant mice.

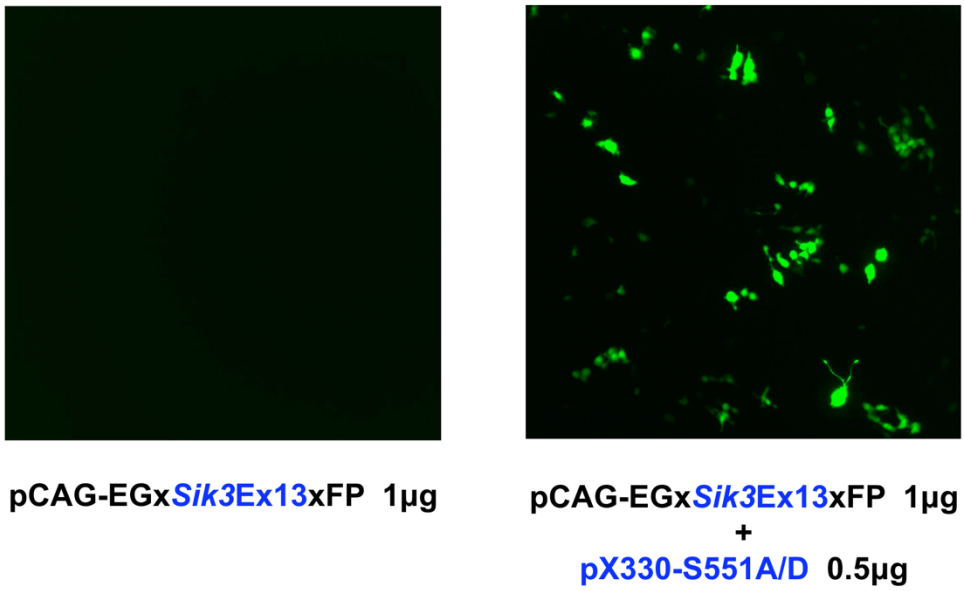

Figure 2. Transfection assay to verify the CRISPR vector

Establishment of *S551A* and *S551D* mutants by CRISPR/Cas9 system

Based on the CRISPR-driven point mutations in the Ser551 region in the *Sik3* gene, we obtained F0 generation mice in a total of 3 heterozygous *S551A* mutants, 6 heterozygous *S551D* mutants, and 2 homozygous *S551D* mutant mice (Figure 3), as confirmed by sequencing analysis. We checked their genomic sequences and confirmed that the 11 mutants had no *Cas9* transgene and no off-target mutations. By genetic crossing with wild-type C57BL/6N female mice, we obtained F1 mice and confirmed the

heritability of the mutations. To analyze the sleep/wake behaviors, we crossed F1 mice with wild-type C57BL/B6N mice. Since the homozygous *S551A* and *S551D* mice were rarely obtained by natural mating, heterozygous F2 mice were used for further experiments and subjected to EEG/EMG recording.

Results : CRISPR engineered F0 mice

line	Injected	Transplant	Birth	m/+	m/m	Total # mutant mice	Success Mutation(%)
Ser→Ala 1 base change	381	350	83	3	0	3	3.6
Ser→Asp 3 bases changes	363	331	78	6	2	8	10

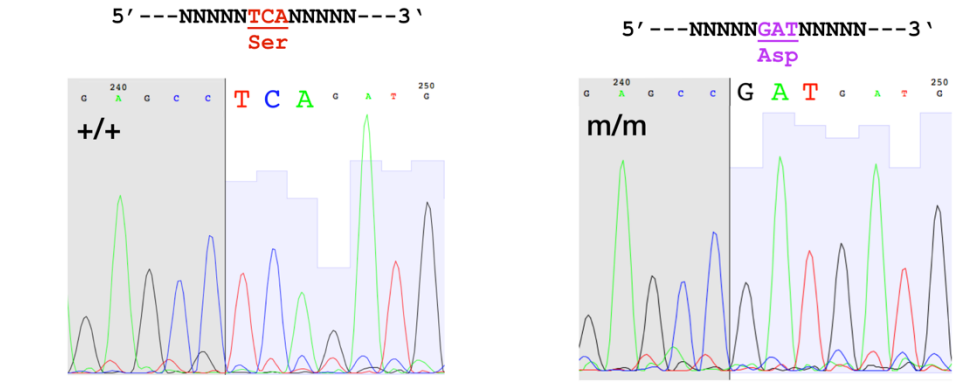

Figure 3. Results of CRISPR/Cas9-based genome editing

Normal transcription and translation of *Sik3* in *S551A/D* mutants

To confirm whether the obtained *S551A* and *S551D* mutant mice showed the normal transcription of *Sik3* gene, we performed reverse transcription PCR (RT-PCR) and quantitative PCR (qPCR) using the extracted mRNA from the cortex tissue of wild-type (WT), *Sleepy* (*ΔEx13*), *S551A*, and *S551D* mice. As previously reported (Funato H, Honda T, Yanagisawa M et al., *Nature* 2016), the size of the transcribed mRNA of heterozygous and homozygous *Sleepy* (*ΔEx13*) mutants was altered owing to the skipped exon 13 (Figure 4). However, both *S551A* and *S551D* mutants showed the same transcriptional patterns of *Sik3* mRNA compared to WT mice. In addition, the qPCR results showed that there was no difference in *Sik3* mRNA expression level among littermate WT mice, *S551A* and *S551D* mutants (Figure 5). These data suggested that the transcription of *Sik3* was intact in *S551A* and *S551D* mutants.

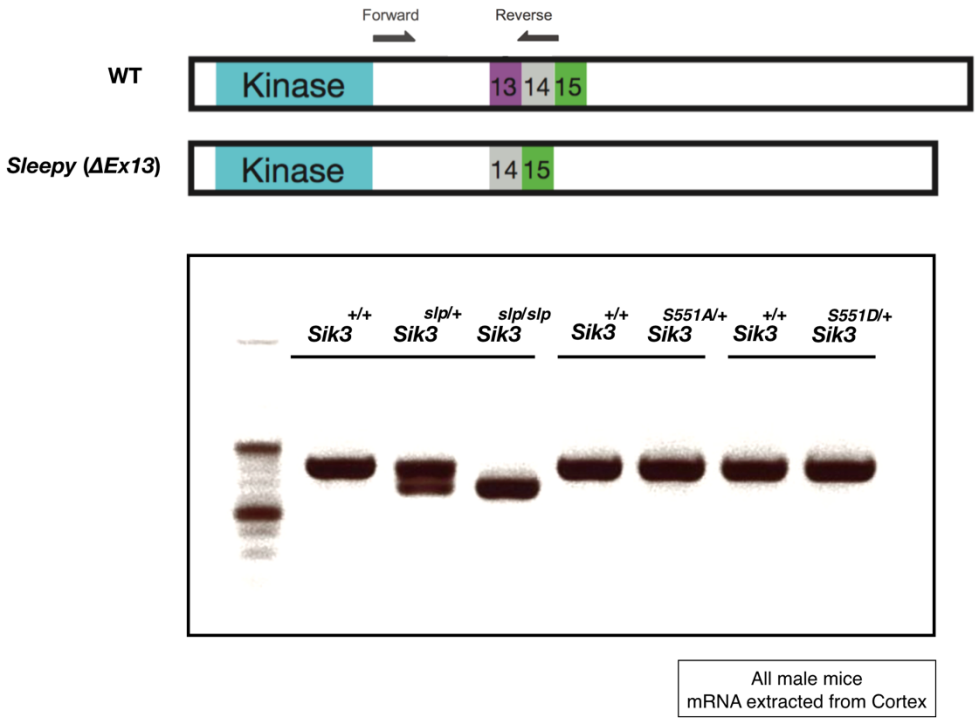

Figure 4. RT-PCR of *S551A* and *S551D* mutant mice

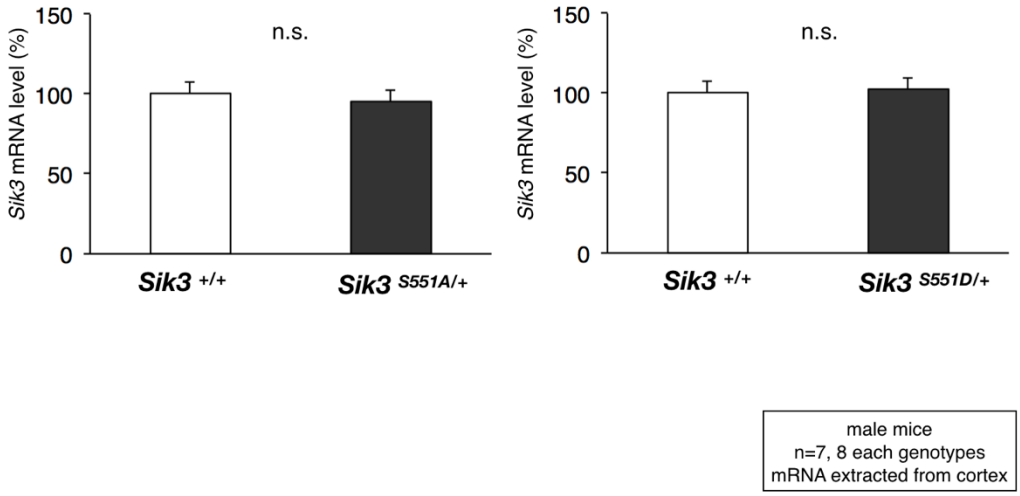

Figure 5. qPCR of *S551A* and *S551D* mutant mice

Two-tailed unpaired *t*-test. Data are presented as the mean ± SEM.

To examine the protein synthesis of *Sik3* in *S551A* and *S551D* mutant mice, we performed western blotting by using an anti-SIK3 antibody that recognizes the C-terminal of SIK3 protein. The half-brain samples were used for western blotting. The anti-SIK3 antibody detected the same size of SIK3 protein in both *S551A* and *S551D* mutant (Figure 6) compared with WT littermate mice. This result showed normal protein synthesis of the *Sik3* gene in *S551A* and *S551D* mutants. Taking these results together, we confirmed that the single amino acid changes in the Ser551 region had no effect on the transcription or translation of the *Sik3* gene.

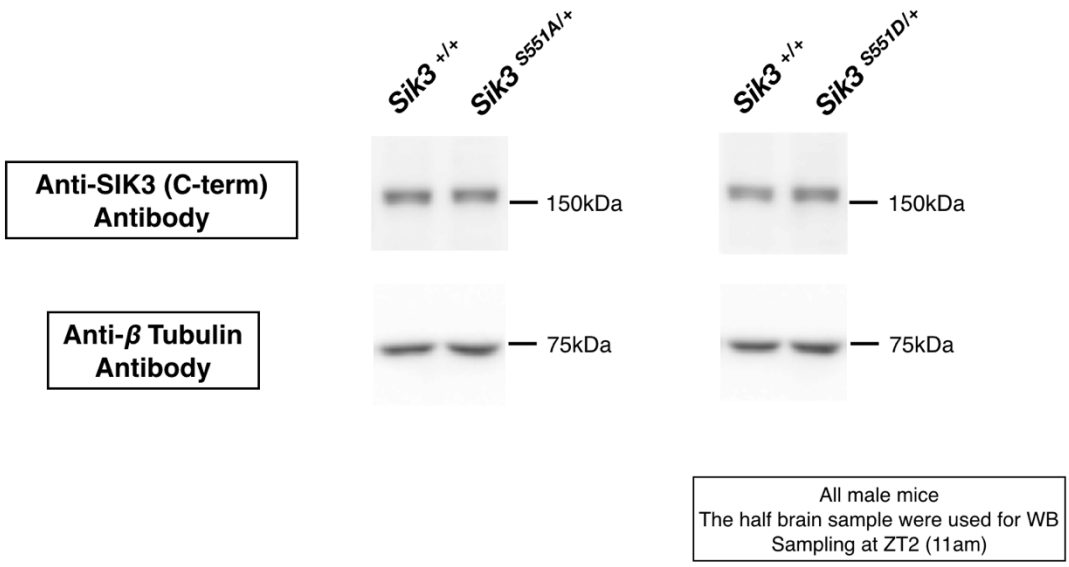

Figure 6. SIK3 protein synthesis of *S551A* and *S551D* mutants

***Ser551Ala* mutation in *Sik3* increased NREMS amount**

S551A mutants exhibited a reduced wake amount and an increased NREMS amount in both the light and dark phases (Figure 7A), but the hypersomnia phenotype was more prominent in the dark phase (Figure 7B). The opposite effect was observed for wakefulness: *S551A* mutants displayed decreased wakefulness in both the light and dark phases (Figure 7A). In contrast, there was no difference in total REMS amount over 24 hours, suggesting that the NREMS-specific change occurs in *S551A* mutants.

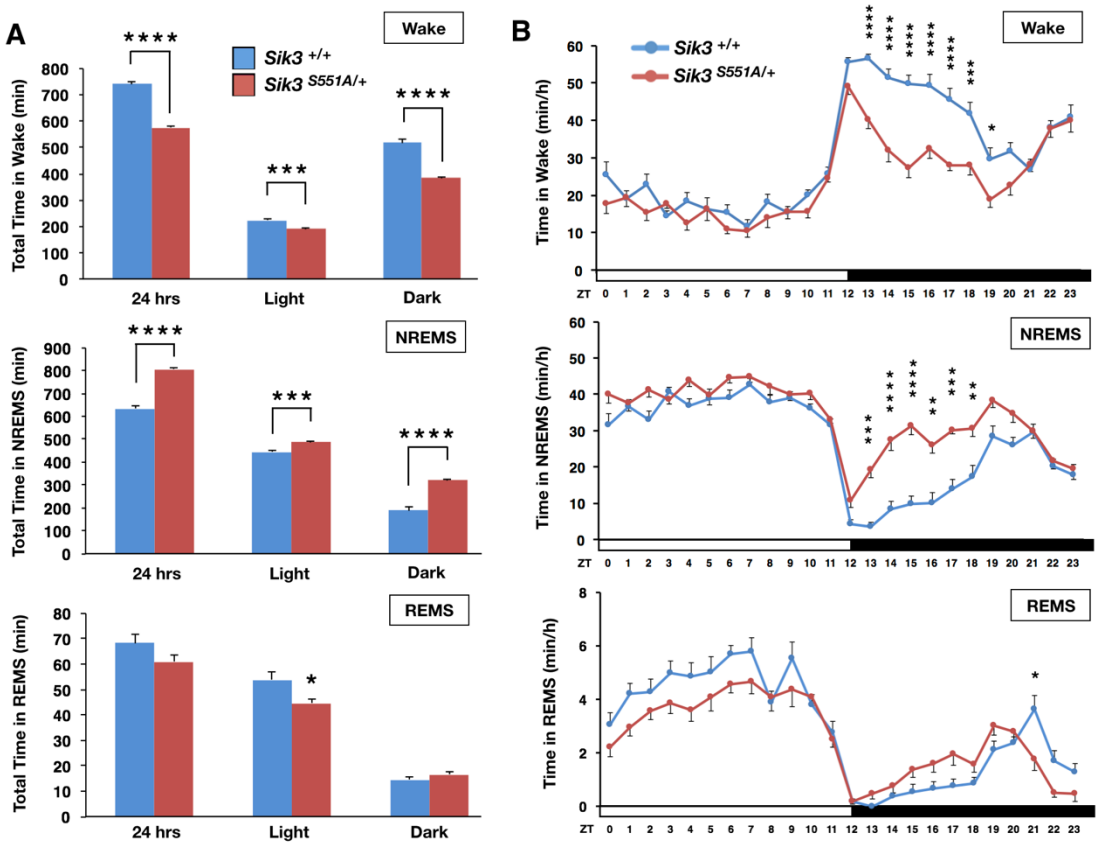

Figure 7. Sleep/wake phenotype of *S551A* mutant mice

(A) Total time in wakefulness, NREMS, REMS. n = 14 for each genotype. *P < 0.05, ***P < 0.001, ****P < 0.0001, two-tailed unpaired t-test (B) Circadian variation in wakefulness, NREMS and REMS. n = 14 for each genotype. *P < 0.05, **P < 0.01, ***P < 0.001, ****P < 0.0001, two-way repeated measure ANOVA followed by Bonferroni's multiple comparisons test. Wake: the main effect of genotype, F (1, 26) = 143.8, ****P < 0.0001. NREMS: the main effect of genotype, F (1, 26) = 126, ****P < 0.0001.

REMS: the main effect of genotype, F (1, 26) = 2.694, P = 0.1128. NREMS/REMS/Wakefulness stages are assigned in 20-s epochs. Data are presented as the mean ± SEM.

***Ser551Ala* mutation in *Sik3* increased NREMS episode duration**

Moreover, *S551A* mutants exhibited a longer NREMS episode duration in both the light and dark phases, but there was no change in REMS episode duration (Figure 8A). The episode duration of wakefulness was decreased in the dark phase compared with that of the WT littermates (Figure 8A). These results were consistent with the longer total NREMS amount and shorter total wake amount in *S551A* mutants. For the transitions to wakefulness, NREMS, and REMS over 24 hours, *S551A* mutants showed a reduced number of transitions from NREMS to REMS (Figure 8B). This result suggests that *S551A* mutants tended to stay in NREM state longer than the WT did, which was consistent with the increased NREMS amount.

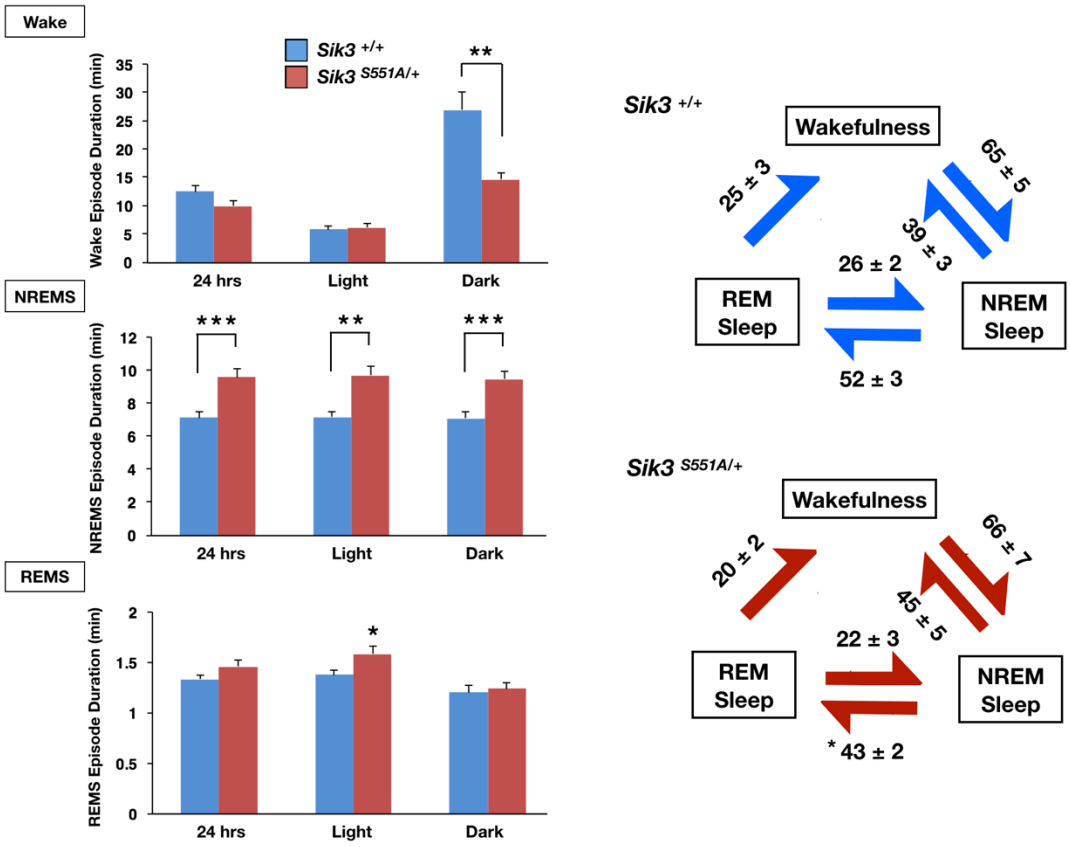

Figure 8. Sleep/wake episode durations and transitions of *S551A* mutants

n = 14 for each genotype. *P < 0.05 **P < 0.01 ***P < 0.001, two-tailed unpaired t-test and Mann-Whitney U-test. NREMS/REMS/Wakefulness stages are assigned in 20-s epochs. Data are presented as the mean ± SEM.

Increased sleep need in *S551A* mice with increased delta power density

The EEG spectral analysis of *S551A* mice during wakefulness, NREMS, and REMS revealed that the EEG power density in the delta frequency

range (1–4 Hz) during NREMS (known as a marker of sleep need) was significantly increased in *S551A* mutants over 24 hours compared with that of the WT littermates (Figure 9). This result suggests that the baseline sleep need was inherently increased in the *S551A* mutants.

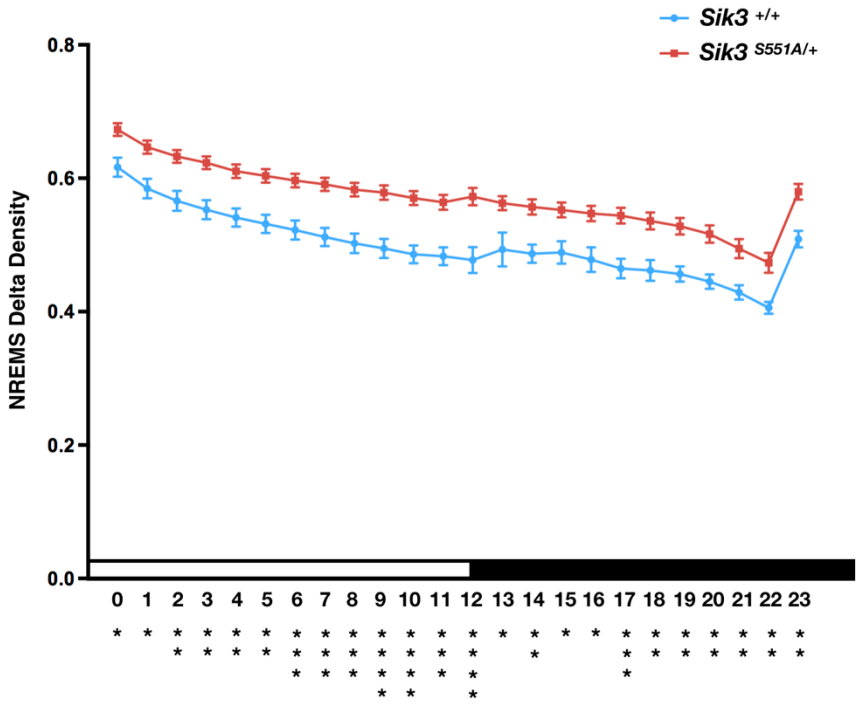

Figure 9. NREMS delta power density of *S551A* mutants

$n = 14$ for each genotype. *$P < 0.05$, **$P < 0.01$, ***$P < 0.001$, ****$P < 0.0001$, two-way repeated measure ANOVA followed by Bonferroni's multiple comparisons test. The main effect of genotype, $F(1, 26) = 19.223$,

***P = 0.0002. NREMS/REMS/Wakefulness stages are assigned in 20-s epochs. Data are presented as the mean ± SEM.

Importantly, the sleep/wake phenotypes of *S551A* mice with an increased NREMS amount, longer NREMS episode duration and higher sleep need were consistent with the phenotypes of the ENU-based original *Sleepy* (*ΔEx13*) mutant pedigree (Funato H, Honda T, Yanagisawa M et al., *Nature* 2016). This result indicates that the single amino acid change at Ser551, Ser551Ala mutation, was sufficient to induce the phenotypes of the *Sleepy* mutants with the skipped exon 13. This finding suggests that the Ser551 in exon 13 of *Sik3* gene plays a crucial role in maintaining the normal amount of sleep.

The EEG spectral analysis of *S551A* mutant mice during wakefulness showed prominently increased low-frequency power density in delta range (1–7 Hz) (Figure 10). This result suggests the possible association between

increased sleep need and the local sleep state in cortical regions (Vyazovskiy VV et al., *Nature* 2011) and may reflects that *S551A* mutants suffer from sleepiness even during wakefulness. This may associate with the decreased episode duration of wakefulness during dark period (Figure 8). For NREMS, *S551A* mutant mice showed increased power density in delta range (1–4 Hz) (Figure 10). For REMS, the EEG power density in theta range (6–7 Hz) was increased in *S551A* mutant mice (Figure 10).

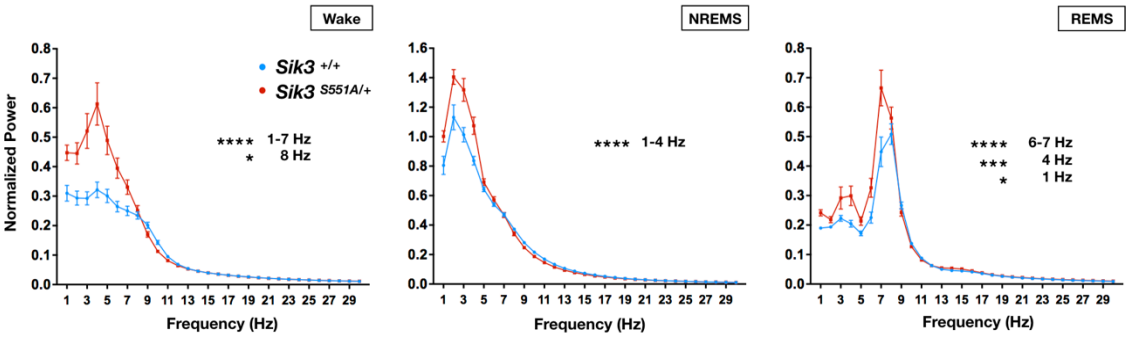

Figure 10. EEG power spectra of *S551A* mutants

n = 14 for each genotype. *P < 0.05, ***P < 0.001, ****P < 0.0001, two-way repeated measure ANOVA followed by Bonferroni's multiple comparisons test. Wake: the main effect of genotype, F (1, 26) = 10.83, **P = 0.0029. NREMS: the main effect of genotype, F (1, 26) = 8.521, **P

= 0.0072. REMS: the main effect of genotype, F (1, 26) = 5.978, *P = 0.0216. NREMS/REMS/Wakefulness stages are assigned in 20-s epochs. Data are presented as the mean ± SEM.

***Ser551Asp* mutation in *Sik3* increased NREMS amount**

S551D mutants exhibited reduced wake amount and increased NREMS amount in both the light and dark phases (Figure 11A) which is similar to the phenotypes of *S551A* mutants. In parallel, *S551D* mutants displayed decreased wakefulness in both the light and dark phases (Figure 11B). However, there was no difference in the total REMS amount over 24 hours, indicating that the NREMS-specific change was found only in *S551D* mutants.

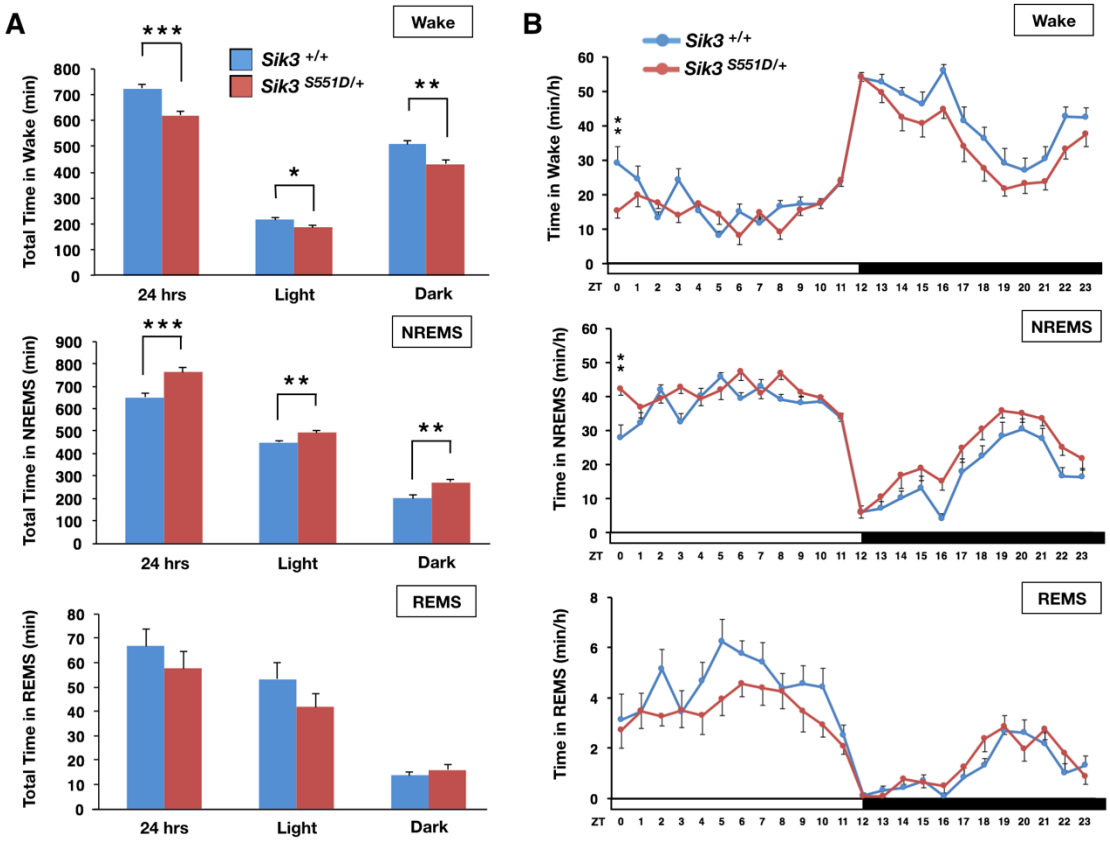

Figure 11. Sleep/wake phenotype of *S551D* mutant mice

(A) Total amount in wakefulness, NREMS, REMS. n = 10 for each genotype. *P < 0.05, **P < 0.01, ***P < 0.001, two-tailed unpaired t-test and Mann-Whitney U-test. (B) Circadian variation in wakefulness, NREMS, and REMS. n = 10 for each genotype. **P < 0.01, two-way repeated measure ANOVA followed by Bonferroni's multiple comparisons test. Wake: the main effect of genotype, F (1, 18) = 16.06, ***P < 0.001. NREMS: the main effect of genotype, F (1, 18) = 17.15, ***P < 0.001.

REMS: the main effect of genotype, F (1, 18) = 0.7886, P = 0.3862. NREMS/REMS/Wakefulness stages are assigned in 20-s epochs. Data are presented as the mean ± SEM.

***Ser551Asp* mutation in *Sik3* decreased wake episode duration**

In addition, *S551D* mutants displayed shorter wake episode duration in the dark phase but no change in REMS episode duration (Figure 12A). The episode duration of NREMS tended to increase, but no significant difference was observed compared with the WT littermates (Figure 12A). For the transitions to wakefulness, NREMS, and REMS over 24 hours, *S551D* showed no changes in the transition profiles compared to WT littermate mice (Figure 12B).

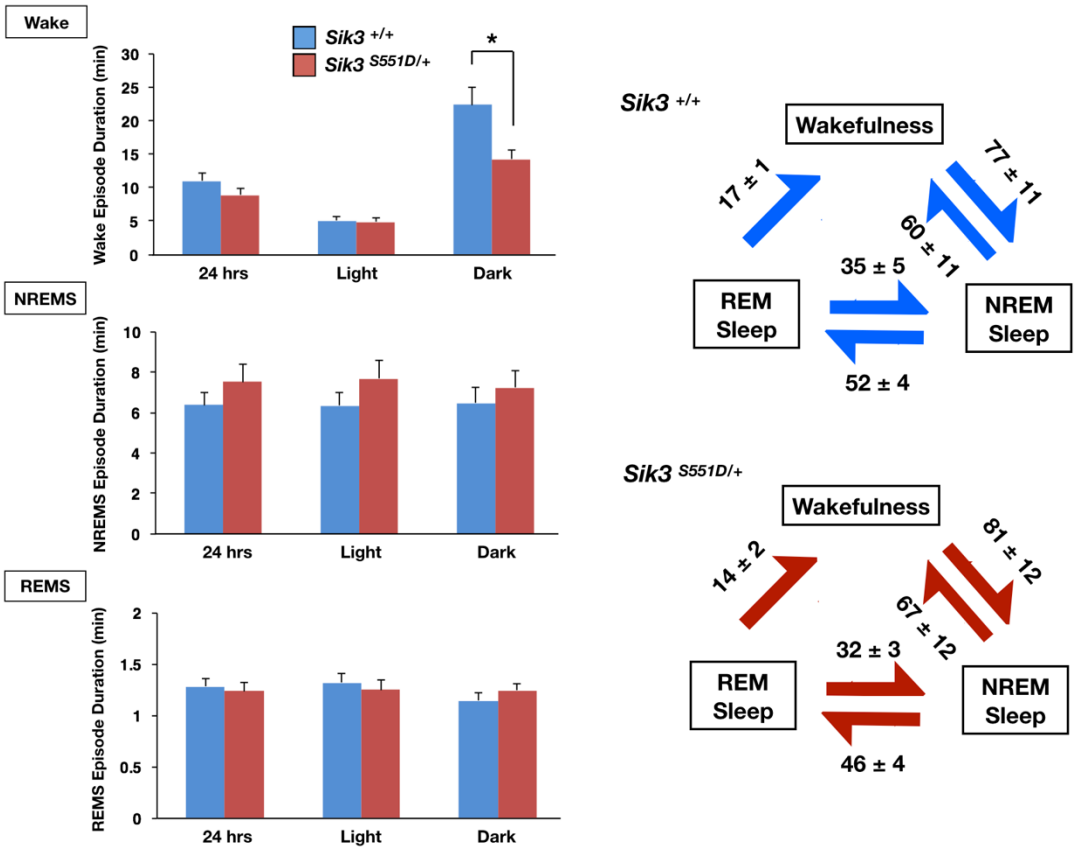

Figure 12. Sleep/wake episode durations and transitions of *S551D* mutants $n = 10$ for each genotype. $*P < 0.05$, two-tailed unpaired *t*-test and Mann-Whitney *U*-test. NREMS/REMS/Wakefulness stages are assigned in 20-s epochs. Data are presented as the mean ± SEM.

Increased sleep need in *S551D* mice with increased delta power density

The EEG spectral profile of *S551D* mutants during NREMS showed increased power density in the delta (1-4 Hz) frequency range compared

with the WT littermates (Figure 13). This result suggests that the baseline sleep need of *S551D* mutants was inherently increased.

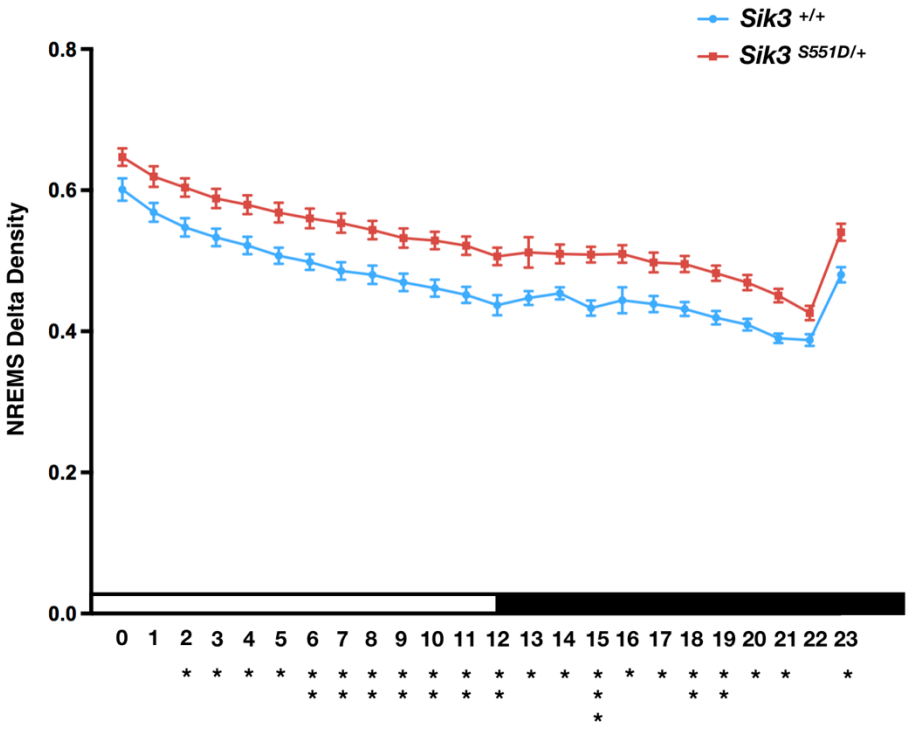

Figure 13. NREMS delta power density of *S551D* mutants

n = 10 for each genotype. *P < 0.05, **P < 0.01, ***P < 0.001, two-way repeated measure ANOVA followed by Bonferroni's multiple comparisons test. The main effect of genotype, F (1, 18) = 14.285, **P = 0.0014. NREMS/REMS/Wakefulness stages are assigned in 20-s epochs. Data are presented as the mean ± SEM.

The EEG spectral analysis of *S551D* mutant mice during wakefulness showed prominently increased low-frequency power density in delta range (1–4 Hz) (Figure 14) which is similar to the phenotypes of *S551A* mutants. For NREMS, *S551D* mutant mice showed increased power density in delta range (1–3 Hz) (Figure 14). For REMS, the EEG power density in theta range (7 Hz) was increased in *S551D* mutant mice (Figure 14).

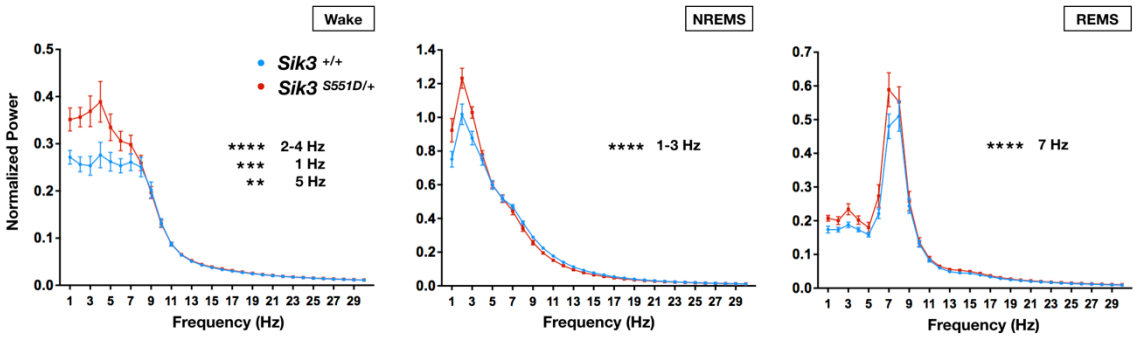

Figure 14. EEG power spectra of *S551A* mutants

n = 10 for each genotype. $^{**}P < 0.01$, $^{***}P < 0.001$, $^{****}P < 0.0001$, two-way repeated measure ANOVA followed by Bonferroni's multiple comparisons test. Wake: the main effect of genotype, F (1, 18) = 6.562, $^{*}P$ = 0.0196. NREMS: the main effect of genotype, F (1, 18) = 1.459, P = 0.2427. REMS: the main effect of genotype, F (1, 18) = 4.451, $^{*}P$ = 0.0491.

NREMS/REMS/Wakefulness stages are assigned in 20-s epochs. Data are presented as the mean ± SEM.

Although the detailed characteristics, such as the profile of episode durations and detailed EEG spectra, are different, *S551D* mutants clearly showed increased NREMS amount, decreased wakefulness amount over 24 hours and increased NREMS delta power density with a higher sleep need, similar to the *S551A* and the ENU-based *Sleepy* (*ΔEx13*) mutants.

This finding raised the possibility that the existence of a Serine residue at the 551 position as the phosphorylation target from the upstream PKA could play an important role in normal sleep/wake regulation. In other words, there is a possibility that the intracellular signaling pathway through the protein-protein interaction between PKA and SIK3 (determined by Ser551) could be altered by mutations in the Ser551 region compared with the normal physiological condition. To examine how the mutations in the

Ser551 region affect the SIK3 signaling pathway and its binding partners, we performed a series of biochemical analyses. These biochemical experiments are essential not only to examine the molecular mechanisms of similar sleep/wake phenotypes among *S551A, S551D,* and *Sleepy (ΔEx13*) mutants but also to reveal the core intercellular signaling pathway that connects the cellular events to the dynamic *in vivo* sleep/wake behaviors.

Although few studies have reported the binding partners of SIK3, several candidate partners are known. It has been reported that SIK3 is regulated by the LKB1 (liver kinase B1: serine/threonine kinase 11) phosphorylation of a threonine residue T221 in the activation of T-loops (Lizcano JM, et al. *EMBO J* 2004). T221 is closely associated with the kinase activity of SIK3 (Katoh Y, et al. *FEBS J* 2006; Berggreen C, et al. *Cell Signal* 2012). It has also been reported that cAMP-elevation induces a PKA-dependent phosphorylation of SIK3 that depends on T469, S551, S674 and subsequently increased binding to the 14-3-3 protein (Berggreen

C, et al. *Cell Signal* 2012). Since *S551A, S551D, Sleepy (ΔEx13*) mutants have mutations or deletions in the Ser551 region, we focused on the interactions toward PKA and 14-3-3 in further biochemical analyses.

Mutations at Ser551 altered the binding pattern of the SIK3 protein

We constructed the pcDNA-based HA-*Sik3* (WT), HA-*S551A*, HA-*S551D*, and HA-*Sleepy* (*ΔEx13*) expression plasmids and then individually transfected them into HEK293 cells. After immunoprecipitation (IP) with anti-HA antibody, western blotting was performed by using the corresponding antibodies that bound to the target molecules.

To confirm the transfection quality, we first used the custom-made anti-SIK3 (Ex13) antibody, which recognizes 14 amino acids in the middle of exon 13. The basal expression of SIK3 protein was confirmed by using anti-HA antibody. HA-*Sik3* (WT), HA-*S551A* and HA-*S551D* displayed the

same band size (Figure 15) when using the anti-HA antibody. Only HA-*Sleepy* (*ΔEx13*) showed an altered band size because of the skipped exon 13, as previously reported (Funato H, Honda T, Yanagisawa M et al., *Nature* 2016). As a negative control, HEK293 cells with no plasmid transfection were used to show blank expression. The anti-SIK3 (Ex13) antibody detected the same size and amount of SIK3 protein in HA-*Sik3* (WT), HA-*S551A* and HA-*S551D* but not in HA-*Sleepy* (*ΔEx13*). This result suggests the anti-SIK3 (Ex13) antibody worked precisely to detect the sufficient expression of WT and mutant SIK3 proteins and the existence of exon 13 in the synthesized SIK3 protein.

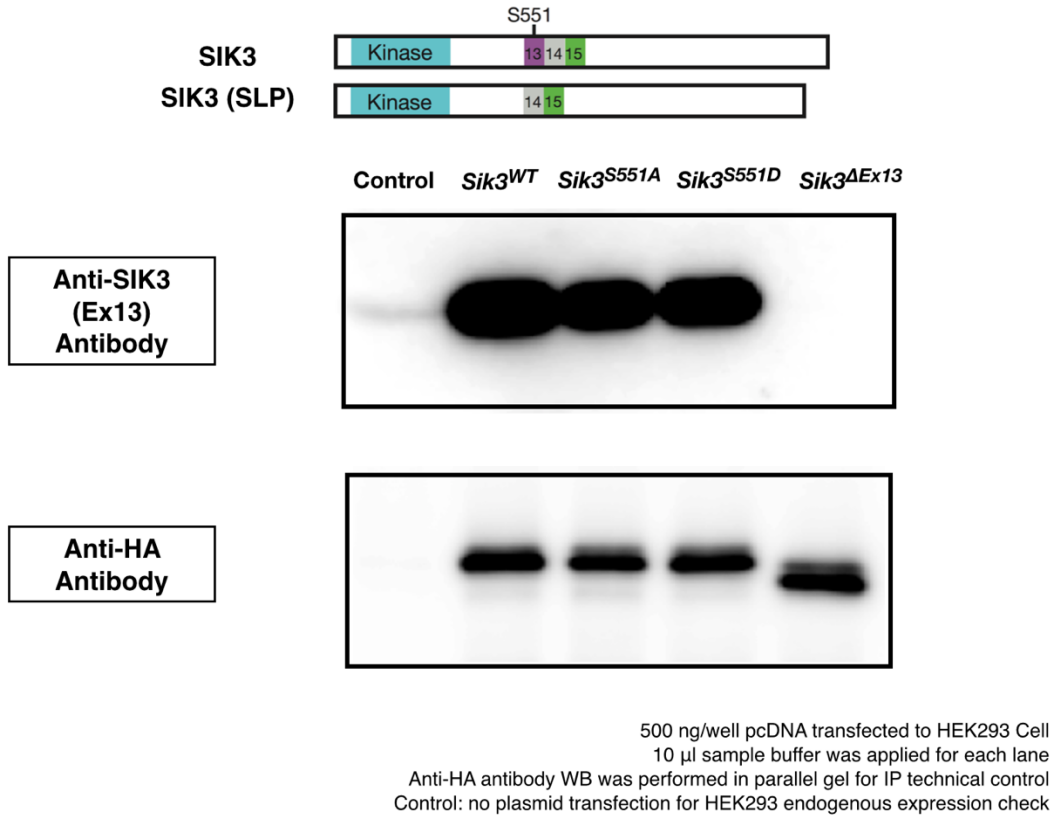

Figure 15. IP-WB result using anti-SIK3 (Ex13) antibody

We next examined how the mutations or deletion at Ser551 in the *Sik3* gene affect the recognition from PKA protein, which is upstream of SIK3. We used the phospho-PKA substrate antibody, which detects the substrates of PKA containing a phospho-PKA substrate motif with phospho-Ser/Thr residue. By contrast with HA-*Sik3* (WT), the mutant lines HA-*S551A*, HA-*S551D* and HA-*Sleepy* (*ΔEx13*) all showed similarly decreased binding

to the phospho-PKA substrate antibody (Figure 16). This result suggests that the SIK3 proteins with the *S551A*, *S551D* and *Sleepy* (*ΔEx13*) mutations are excluded from the possible substrates of PKA. The consistency of binding patterns among these mutants corresponded to their similar hypersomnia phenotypes with prolonged NREM sleep.

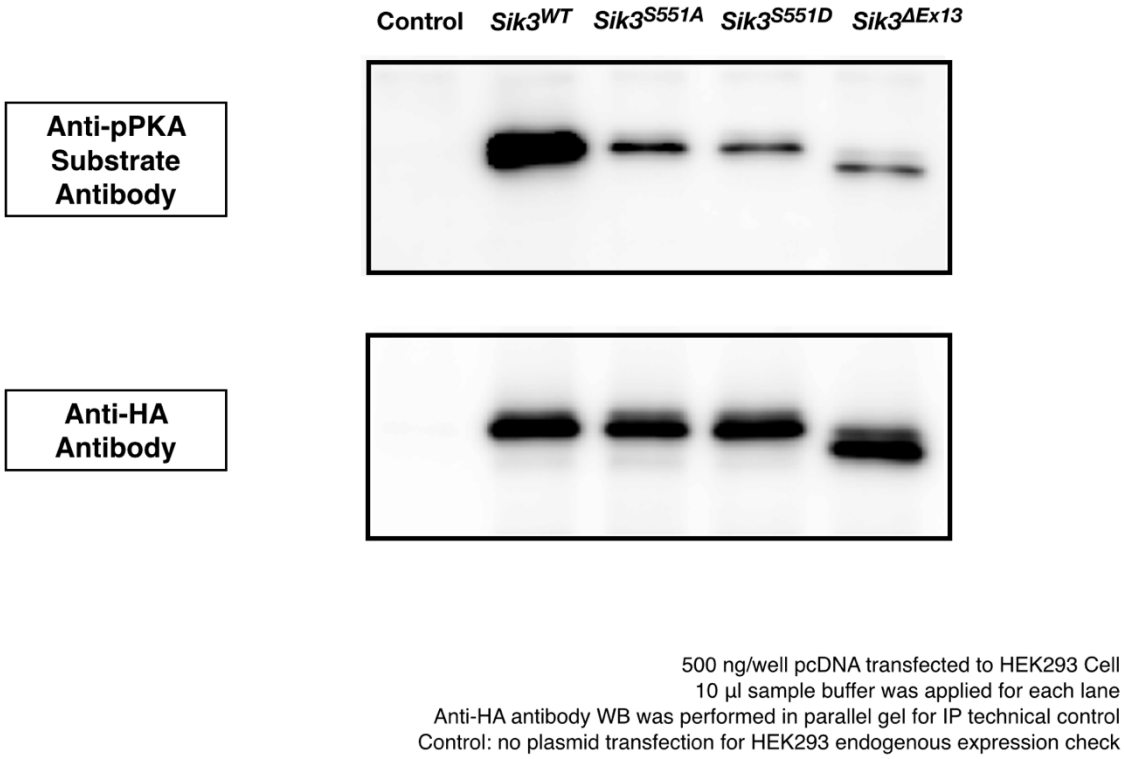

Figure 16. IP-WB result using anti-pPKA substrate antibody

Similar to the binding patterns of the phospho-PKA substrate antibody, the anti-14-3-3 antibody detected clear band expression in HA-*Sik3* (WT) but no binding in HA-*S551A*, HA-*S551D* and HA-*Sleepy* (*ΔEx13*) (Figure 17). These results clearly demonstrated that the three mutations (Ser551Ala, Ser551Asp, Ex13 deletion) abolished the bindings to the 14-3-3 protein.

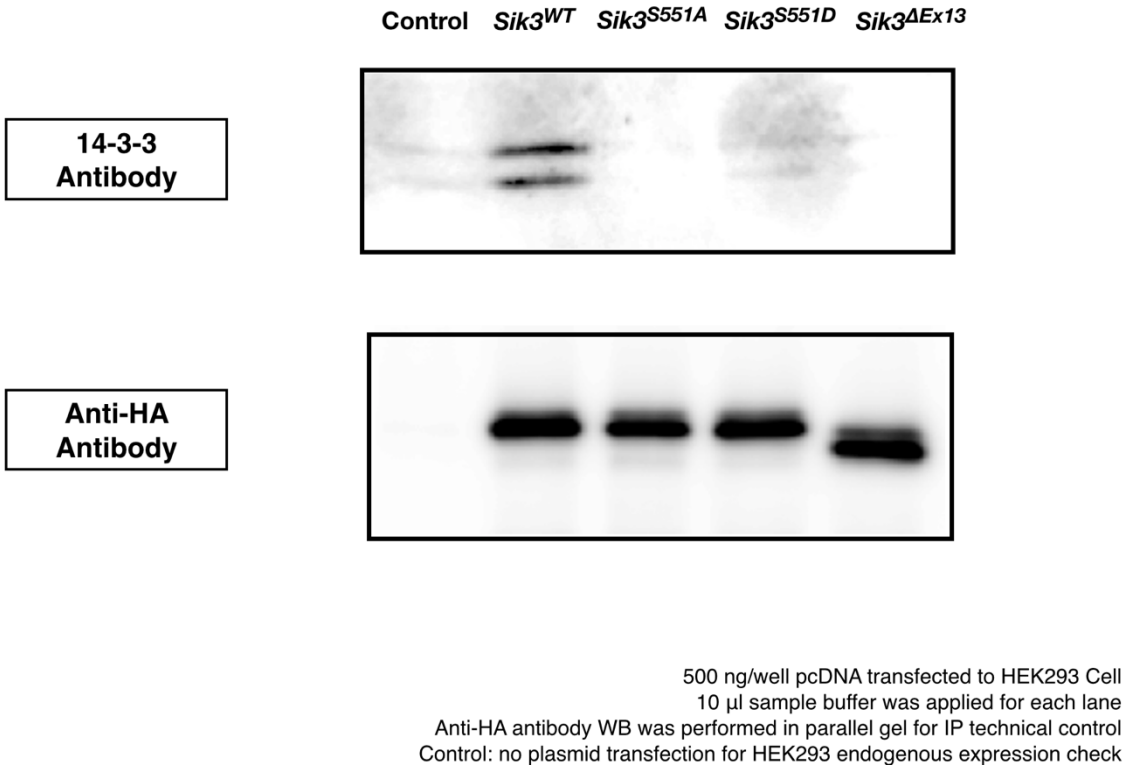

Figure 17. IP-WB result using anti-14-3-3 antibody

Discussion

Through our unique forward genetic screening, we established a *Sleepy* mutant with a hypersomnia phenotype that also had a higher sleep need due to the skipped exon 13 in the *Sik3* gene (Funato H, Honda T, Yanagisawa M et al., *Nature* 2016). In this study, we further revealed that the PKA recognition site Ser551 in the skipped exon 13 had a critical role in regulating the daily sleep amount and sleep need. As previously reported, the Ser551 region is evolutionally conserved in invertebrates, including *D. melanogaster* and *C. elegans*. In both species, *Sik3* orthologues are involved in the regulation of sleep-like behavior (Funato H, Honda T, Yanagisawa M et al., *Nature* 2016). Here, we demonstrated that Ser551 is an essential component for sleep/wake regulation across animal species.

The *S551A* mutants exhibited markedly prolonged NREMS and short wakefulness amounts owing to the increased NREMS episode duration and the decreased wake episode duration. Importantly, *S551A* mutants also

exhibited increased NREMS delta power density, an index of homeostatic sleep need, and longer NREMS episode duration. In addition to NREMS delta power density, NREMS episode duration has been considered a marker of sleep need (Bjorness TE, et al. *J Neurosci* 2016). Together, these results demonstrated that *S551A* mutants have an inherently higher sleep need. These results also suggest that the Ser551Ala (*S551A*) mutation was sufficient to induce the phenotypes of ENU-based original *Sleepy* (*ΔEx13*) mutant. Additionally, Ser551Asp (*S551D*) mutants also exhibited prolonged NREMS amount and increased NREMS delta power density compared with these of WT mice. Taking these findings together, we found that the mutations or deletion of Ser551 in the *Sik3* gene caused prolonged NREMS amount and increased sleep need *in vivo*, suggesting the existence of Ser551, a PKA recognition site, is crucial for normal sleep/wake regulation and maintenance of daily sleep need.

At the molecular level, through IP and western-blotting, we confirmed that *Sleepy* (*ΔEx13*), *S551A*, and *S551D* mutants showed decreased binding

to the phospho-PKA substrate antibody. This result strongly suggests that the SIK3 proteins with *S551A*, *S551D* and *Sleepy* (*ΔEx13*) mutations are excluded from the possible substrates of PKA. These three mutants also showed abolished bindings to 14-3-3, which corresponded to their consistent hypersomnia phenotypes with prolonged NREM sleep. This raises the possibility that the deletion or mutations at Ser551 caused the disrupted recognition from the upstream PKA and resulted in the loss of binding to 14-3-3. A recent study also reported that loss of either of two 14-3-3 binding sites in SIK3 abolished 14-3-3 association, and rendered SIK3 insensitive to cAMP signaling in a cell-based CRE reporter assay (Sonntag T, et al. *FEBS J* 2018). This study, taken together with our results, raises the possibility that *Sleepy* (*ΔEx13*), *S551A* and *S551D* mutations may cause the conformational changes and affect the interactions of SIK3 toward the intrinsic binding partners and downstream targets, such as cAMP-regulated transcriptional coactivators (CRTCs) and Class IIA histone deacetylases (HDACs) following the abolished 14-3-3 association.

Our results of *in vivo* sleep phenotypes suggest that the existence of Ser551 in the *Sik3* gene and its signaling pathway, including PKA and 14-3-3, may play a key role in sleep/wake regulation under normal physiological conditions (Figure 18). Notably, the exon 13-encoding region of *Sik3*, including Ser551, is highly conserved among both vertebrates and invertebrates, which suggests the biological importance of the phosphorylation pathway PKA / SIK3 / 14-3-3 in sleep/wake regulation. These findings provide landmark information about novel sleep/wake regulatory mechanisms by connecting the intracellular signaling pathway to dynamic *in vivo* sleep/wake behaviors.

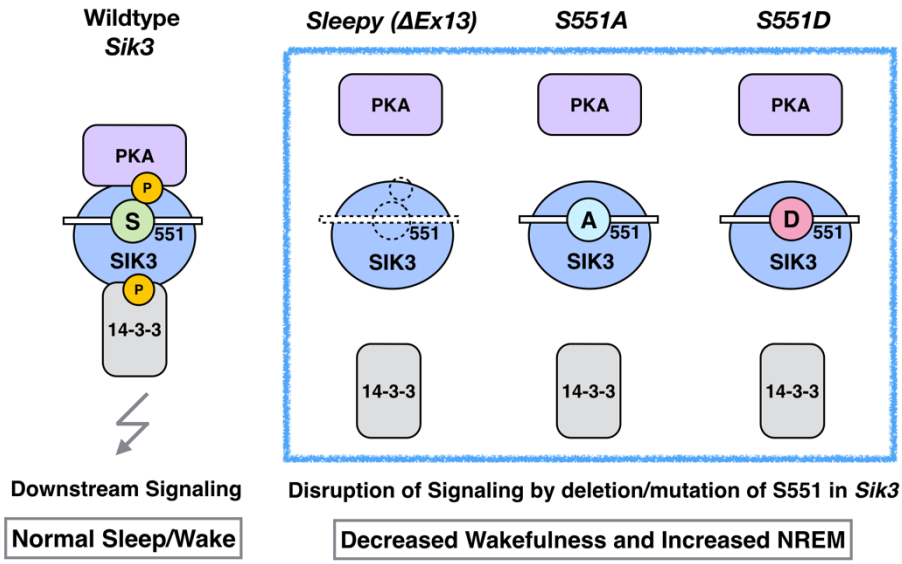

Figure 18. Intercellular signaling pathway regulating sleep/wake behavior

Acknowledgements

We thank all Yanagisawa/Funato laboratory and WPI-IIIS members, especially Dr. M. Yanagisawa, Dr. H. Funato, Dr. C. Miyoshi, Dr. T. Fujiyama, Ms. A. Ikkyu, Ms. N. Hotta-Hirashima and Ms. S. Kanno for their kind support and advice on this project. We thank Dr. M. Lazarus, Dr. JS. Takahashi and Dr. S. Mizuno for the critical comments and suggestions on this project. We also thank Dr. S. Takahashi and Dr. S. Mizuno for the support on generation of CRISPR engineered mice. This work was supported by JSPS KAKENHI (grant number 15J06369 to T. Honda; 26220207 and 17H06095 to M. Yanagisawa and H. Funato) and the World Premier International Research Center Initiative from MEXT to M. Yanagisawa.

References

1. Funato H, Miyoshi C, Fujiyama T, Kanda T, Sato M, Wang Z, Ma J, Nakane S, Tomita J, Ikkyu A, Kakizaki M, Hotta-Hirashima N, Kanno S,

Komiya H, Asano F, Honda T, Kim SJ, Harano K, Muramoto H, Yonezawa T, Mizuno S, Miyazaki S, Connor L, Kumar V, Miura I, Suzuki T, Watanabe A, Abe M, Sugiyama F, Takahashi S, Sakimura K, Hayashi Y, Liu Q, Kume K, Wakana S, Takahashi JS, Yanagisawa M. Forward-genetics analysis of sleep in randomly mutagenized mice. *Nature*. 2016 539(7629):378-383.

2. Honda T, Lee CY, Yoshida-Kasikawa M, Honjo K, Furukubo-Tokunaga K. Induction of associative olfactory memory by targeted activation of single olfactory neurons in *Drosophila* larvae. *Sci Rep.* 2014 4:4798.
3. Honda T, Lee CY, Honjo K, Furukubo-Tokunaga K. Artificial Induction of Associative Olfactory Memory by Optogenetic and Thermogenetic Activation of Olfactory Sensory Neurons and Octopaminergic Neurons in *Drosophila* Larvae. *Front Behav Neurosci*. 2016 10:137
4. Uchiyama M. Impacts of sleep disorders on human social activities and their economic cost. *J. Jpn. Psychiatr. Hosp. Assoc.* 2012 11:1163
5. Takahashi JS, Shimomura K, Kumar V. Searching for genes underlying

behavior: lessons from circadian rhythms. *Science*. 2008 322(5903): 909-12.

6. Konopka RJ, Benzer S. Clock mutants of Drosophila melanogaster. *Proc Natl Acad Sci U S A.* 1971 68(9):2112-6.

7. Reddy P, Zehring WA, Wheeler DA, Pirrotta V, Hadfield C, Hall JC, Rosbash M. Molecular analysis of the period locus in Drosophila melanogaster and identification of a transcript involved in biological rhythms. *Cell*. 1984 38(3):701-10.

8. Zehring WA, Wheeler DA, Reddy P, Konopka RJ, Kyriacou CP, Rosbash M, Hall JC. P-element transformation with period locus DNA restores rhythmicity to mutant, arrhythmic Drosophila melanogaster. *Cell*. 1984 39(2 Pt 1):369-76.

9. Bargiello TA, Jackson FR, Young MW. Restoration of circadian behavioural rhythms by gene transfer in Drosophila. *Nature*. 1984-1985 312(5996):752-4.

10. Feldman JF, Hoyle MN. Isolation of circadian clock mutants of

Neurospora crassa. *Genetics*. 1973 75(4):605-13.

11. McClung CR, Fox BA, Dunlap JC. The *Neurospora* clock gene frequency shares a sequence element with the *Drosophila* clock gene period. *Nature*. 1989 339(6225):558-62.

12. Vitaterna MH, King DP, Chang AM, Kornhauser JM, Lowrey PL, McDonald JD, Dove WF, Pinto LH, Turek FW, Takahashi JS. Mutagenesis and mapping of a mouse gene, Clock, essential for circadian behavior. *Science*. 1994 264(5159):719-25.

13. King DP, Zhao Y, Sangoram AM, Wilsbacher LD, Tanaka M, Antoch MP, Steeves TD, Vitaterna MH, Kornhauser JM, Lowrey PL, Turek FW, Takahashi JS. Positional cloning of the mouse circadian clock gene. *Cell*. 1997 89(4):641-53.

14. Campbell SS, Tobler I. Animal sleep: a review of sleep duration across phylogeny. *Neurosci Biobehav Rev*. 1984 8(3):269-300.

15. Rial RV, Akaârir M, Gamundí A, Nicolau C, Garau C, Aparicio S, Tejada S, Gené L, González J, De Vera LM, Coenen AM, Barceló P,

Esteban S. Evolution of wakefulness, sleep and hibernation: from reptiles to mammals. *Neurosci Biobehav Rev.* 2010 34(8):1144-60.

16. Hendricks JC, Finn SM, Panckeri KA, Chavkin J, Williams JA, Sehgal A, Pack AI. Rest in Drosophila is a sleep-like state. *Neuron*. 2000 25(1):129-38.
17. Shaw PJ, Cirelli C, Greenspan RJ, Tononi G. Correlates of sleep and waking in *Drosophila* melanogaster. *Science*. 2000 10;287(5459):1834-7.
18. Zhdanova IV, Wang SY, Leclair OU, Danilova NP. Melatonin promotes sleep-like state in zebrafish. *Brain Res*. 2001 903(1-2):263-8.
19. Nath RD, Bedbrook CN, Abrams MJ, Basinger T, Bois JS, Prober DA, Sternberg PW, Gradinaru V, Goentoro L. The Jellyfish *Cassiopea* Exhibits a Sleep-like State. *Curr Biol*. 2017 27(19):2984-2990.e3.
20. Cirelli C, Bushey D, Hill S, Huber R, Kreber R, Ganetzky B, Tononi G. Reduced sleep in Drosophila Shaker mutants. *Nature*. 2005 434(7037):1087-92.

21. Kume K, Kume S, Park SK, Hirsh J, Jackson FR. Dopamine is a regulator of arousal in the fruit fly. *J Neurosci.* 2005 25(32):7377-84.

22. Koh K, Joiner WJ, Wu MN, Yue Z, Smith CJ, Sehgal A. Identification of SLEEPLESS, a novel sleep-promoting factor. *Science*. 2008 321(5887):372-376.

23. Raizen DM, Zimmerman JE, Maycock MH, Ta UD, You YJ, Sundaram MV, Pack AI. Lethargus is a Caenorhabditis elegans sleep-like state. *Nature*. 2008 451(7178):569-72

24. Mashiko D, Fujihara Y, Satouh Y, Miyata H, Isotani A, Ikawa M. Generation of mutant mice by pronuclear injection of circular plasmid expressing Cas9 and single guided RNA. *Sci Rep*. 2013 3:3355.

25. Funato H, Sato M, Sinton CM, Gautron L, Williams SC, Skach A, Elmquist JK, Skoultchi AI, Yanagisawa M. Loss of Goosecoid-like and DiGeorge syndrome critical region 14 in interpeduncular nucleus results in altered regulation of rapid eye movement sleep. *Proc Natl Acad Sci U S A.* 2010 107(42):18155-60.

26. Miyazaki S, Liu CY, Hayashi Y. Sleep in vertebrate and invertebrate animals, and insights into the function and evolution of sleep. *Neurosci Res*. 2017 118:3-12.

27. Vyazovskiy VV, Olcese U, Hanlon EC, Nir Y, Cirelli C, Tononi G. Local sleep in awake rats. *Nature*. 2011 472(7344):443-7.

28. Lizcano JM, Göransson O, Toth R, Deak M, Morrice NA, Boudeau J, Hawley SA, Udd L, Mäkelä TP, Hardie DG, Alessi DR. LKB1 is a master kinase that activates 13 kinases of the AMPK subfamily, including MARK/PAR-1. *EMBO J*. 2004 23(4):833-43.

29. Katoh Y, Takemori H, Lin XZ, Tamura M, Muraoka M, Satoh T, Tsuchiya Y, Min L, Doi J, Miyauchi A, Witters LA, Nakamura H, Okamoto M. Silencing the constitutive active transcription factor CREB by the LKB1-SIK signaling cascade. *FEBS J.* 2006 273(12):2730-48.

30. Berggreen C, Henriksson E, Jones HA, Morrice N, Göransson O. cAMP-elevation mediated by β-adrenergic stimulation inhibits

salt-inducible kinase (SIK) 3 activity in adipocytes. *Cell Signal*. 2012 24(9):1863-71.

31. Bjorness TE, Dale N, Mettlach G, Sonneborn A, Sahin B, Fienberg AA, Yanagisawa M, Bibb JA, Greene RW. An Adenosine-Mediated Glial-Neuronal Circuit for Homeostatic Sleep. *J Neurosci.* 2016 36(13):3709-21.
32. Sonntag T, Vaughan JM, Montminy M, 14-3-3 proteins mediate inhibitory effects of cAMP on salt-inducible kinases (SIKs). *FEBS J*. 2018 285(3):467-480.